Key role of the expression of bone morphogenetic proteins in increasing the osteogenic activity of osteoblast-like cells exposed to shock waves and seeded on bioactive glass-ceramic scaffolds for bone tissue engineering

G. Muzio;G. Martinasso;F. Baino;R. Frairia;C. Vitale-Brovarone;R. A. Canuto. Key role of the expression of bone morphogenetic proteins in increasing the osteogenic activity of osteoblast-like cells exposed to shock waves and seeded on bioactive glass-ceramic scaffolds for bone tissue engineering. JOURNAL OF BIOMATERIALS APPLICATIONS. 29 pp: 728-736.
DOI: 10.1177/0885328214541974

Key role of the expression of bone morphogenetic proteins in increasing the osteogenic activity of osteoblast-like cells exposed to shock waves and seeded on bioactive glass-ceramic scaffolds for bone tissue engineering

Giuliana Muzio[1], Germana Martinasso[1], Francesco Baino[2], Roberto Frairia[3], Chiara Vitale-Brovarone[2], Rosa A. Canuto[1]

[1] *Department of Clinical and Biological Sciences, University of Turin, Corso Raffaello 30, Turin, Italy*

[2] *Institute of Materials physics and Engineering, Department of Applied Science and Technology, Politecnico di Torino, Corso Duca degli Abruzzi 24, Turin, Italy*

[3] *Department of Medical Sciences, University of Turin, Corso Raffaello 30, Turin, Italy*

Corresponding author: Chiara Vitale-Brovarone

Tel.: +39 011 090 4716

Fax: +39 011 090 4624

E-mail: chiara.vitale@polito.it

Abstract

In this work, the role of shock-wave (SW)-induced increase of bone morphogenetic proteins (BMPs) in modulating the osteogenic properties of osteoblast-like cells seeded on a bioactive scaffold was investigated using gremlin as a BMP antagonist. Bone-like glass-ceramic scaffolds, based on a silicate experimental bioactive glass (CEL2) developed at the Politecnico di Torino, were produced by the sponge replication method and used as porous substrates for cell culture.

Human MG-63 cells, exposed to SWs and seeded on the scaffolds, were treated with gremlin every 2 days and analysed after 20 days for the expression of osteoblast differentiation markers. SWs have been shown to induce osteogenic activity mediated by increased expression of alkaline phosphatase, osteocalcin, type I collagen, BMP-4 and BMP-7. Cells exposed to SWs plus gremlin showed increased growth in comparison with cells treated with SWs alone and, conversely, mRNA contents of alkaline phosphatase and osteocalcin were significantly lower. Therefore, the SW-mediated increased expression of BMPs in MG-63 cells seeded on the scaffolds is essential in improving osteogenic activity; blocking BMPs via gremlin completely prevents the increase of alkaline phosphatase and osteocalcin. The results confirmed that the combination of glass-ceramic scaffolds and SWs exposure could be used to significantly improve osteogenesis opening new perspectives for bone regenerative medicine.

Keywords: Scaffold; Shock waves; Gremlin; BMPs; Bone tissue engineering.

Introduction

Tissue engineering represents an interdisciplinary approach to regenerate damaged or diseased tissues through integration of cell biology and biomaterials science. The concept behind tissue engineering is to regenerate target tissue by mimicking the developmental or regenerative process of that tissue; therefore, such an approach can be considered an ideal therapeutic option for treating various tissue defects [1]. Tissue engineering of skin [2], cartilage [3] and bone [4] has already been shown both feasible and effective in several clinical studies, and its efficacy has attracted significant attention from patients, clinicians and biomaterials researchers.

Patients who lose healthy bone tissue as a result of trauma, tumour or inflammation need bone regenerative/reconstructive surgery in order to recover the function of the lost bone. Transplant of an autologous bone graft is the current gold standard to regenerate the lost bone tissue, although this approach is a great burden for patients because autografts must be harvested from a healthy site with the need for extra-surgery and problems of donor site morbidity and pain [5]. Artificial bone substitutes of various origin have been proposed as alternatives to autologous bone [6-8], although bone regeneration with them still exhibit some limitations. For example porous polyethylene, that since the 1990s has been marketed with the commercial name of Medpor® and is widely used in cranio-maxillofacial reconstruction, allows fibrovascular invasion but newly-formed bone does not grow within the polymer porous network due to the lack of both osteo-conductive and osteo-inductive properties [9]. Hydroxyapatite (HA) has been regarded as an ideal bone substitute material due to its chemical and crystallographic similarity with the mineral phase of bone tissue [10], but problems of implant brittleness were observed especially if it is produced in a porous form [11]. Bioactive glasses and glass-ceramics are promising in overcoming the above-mentioned limitations as they can have mechanical properties similar to those of healthy bone [12] and can tightly bond to the host bone creating a stable interface [13].

The development of tissue engineered bioactive glass/cells constructs that could be actually suitable for *in vivo* bone repair is a complex issue requiring the exhaustive knowledge of the artificial materials involved as well as the fine mechanisms of cell osteogenetic activity. A fascinating and new topic of biomedical research aims to understand what stimuli can be provided to cells to promote osteogenesis and, more generally, hard tissue repair. In this regard, shock waves (SWs) are used to treat musculoskeletal disorders, thanks to their efficacy in favouring callus formation in long-bone fractures [14-17]. Despite considerable clinical results and some *in vitro* research, the exact mechanisms underlying SW effect on bone healing still remain unknown. Recently, extracorporeal SW treatment was found to be effective in promoting bone healing (79% success rate) in patients with long-bone non-unions: the effect was found to be associated with systemic elevation of serum NO levels and osteogenic growth factors, including TGF-β1, VEGF and bone morphogenetic protein (BMP)-2 [18]. These observation confirmed the results previously obtained in an animal models by the same research group [19]. *In vitro* studies on human osteoblast-like cells have shown that treatment with SWs influences cell proliferation, enhancing transmembrane currents, as well as the voltage dependence of Ca-activated and K channels [20]. Other studies suggested that exposure to extracorporeal SWs enhances meseoblast recruitment at the junction of ossified cartilage and the production of TGF-β1 and VEGF-A, which are chemotactic and mitogenic, for the recruitment and differentiation of mesenchymal stem cells to promote bone regeneration of segmental defects in rats [21]. More recently, a direct dose-dependent stimulatory effects of SWs on the proliferation and differentiation of osteoblasts from normal human cancellous bone was reported by Hofmann et al. [22]; microarray analysis showed that SW application determines an up-regulation of multiple genes involved in skeletal development and osteoblast differentiation (e.g., PTHrP, prostaglandin E2-receptor EP3, BMP-2 inducible kinase, chordin, cartilage oligomeric matrix protein, matrillin).

Muzio et al. [23] recently demonstrated that SWs initially induce an increase of cell number and osteogenic activity in MG-63 human osteoblast-like cells colonizing bioactive glass scaffolds

(compared to cells untreated with SWs), whereas at a later stage they reduce the number of cells further increasing osteogenic activity, as evidenced by more numerous and larger calcium deposits observed in scaffolds colonized by SW-treated cells. In the same study, a direct effect of SWs on BMP expression was shown for the first time, as it was found that the osteoinductive effect of SWs was mediated by increased expression of ALP, osteocalcin, type I collagen, BMP-4, BMP-7 and BMP-2 [23].

In order to investigate the involvement of increased BMPs expression induced by SWs in modulating the osteogenic properties of human osteoblast-like cells, in this study MG-63 cells were exposed to SWs, seeded on a bioactive glass-ceramic scaffold and for the first time treated with gremlin. Gremlin is a secreted BMP antagonist that is well-known to be mainly involved in the initiation of osteoblast differentiation [24] In this research the effect of gremlin was examined only at 20 days since in our previous study [23] the major differentiation of osteoblasts treated with SWs and seeded on the scaffold was present at this experimental time. This topic is interesting in view of the development of ever more effective strategies to treat bone diseases via the tissue engineering approach.

Materials and methods

Macroporous scaffolds

Synthesis of the starting glass

Foam-like macroporous scaffolds were produced using a 6-oxides silica-based experimental glass (CEL2; 45SiO_2-3P_2O_5-26CaO-15Na_2O-7MgO-4K_2O mol.%) as a starting material. The glass was originally developed by Vitale-Brovarone and co-workers at the Politecnico di Torino for bone tissue engineering applications [25]. CEL2 reagents (high-purity powders of SiO_2, $Ca_3(PO_4)_2$,

$CaCO_3$, Na_2CO_3, $(MgCO_3)_4 \cdot Mg(OH)_2 \cdot 5H_2O$, K_2CO_3 purchased from Sigma-Aldrich) were molten in a platinum crucible at 1500 °C for 1 h in air; the melt was quenched in cold water to obtain a frit, that was subsequently ground by using a 6-balls zirconia milling jar and sieved (Giuliani stainless steel sieve) to obtain particles with size below 32 μm.

Scaffolds fabrication

The scaffolds were produced by the sponge replication method, that was shown to be very effective to obtain porous ceramics with a highly-interconnected 3-D network of open macropores [26]. Small cubic blocks (15.0 mm × 15.0 mm × 15.0 mm) of a commercial open-cells polyurethane (PU) sponge (density of the porous polymer ~20 kg m^{-3}) were coated with CEL2 powder by being impregnated in a water-based glass slurry (glass : distilled water : poly(vinyl alcohol) (PVA) = 30 : 64 : 6 wt.%). After PVA hydrolysis under continuous magnetic stirring at 80 °C, CEL2 powder was added to the solution; the water evaporated during PVA dissolution was re-added to the slurry to restore the correct weight ratios among the components. After further stirring for 15 minutes at room temperature to ensure slurry homogeneity, the sponge blocks were immersed for 60 s in the slurry. The slurry infiltrated the porous network of the PU template that was extracted from the slurry and subsequently compressed (20 kPa for 1 s) up to 60% in thickness along three orthogonal spatial directions, in order to homogeneously remove the excess slurry. The samples were dried at room temperature overnight and afterwards thermally treated at 950 °C for 3 h (heating and cooling rates set at 5 and 10 °C min^{-1}, respectively) in order to burn-off the polymeric template and to sinter the inorganic particles. As reported elsewhere [26], two crystalline silicate phases develop during the above-mentioned heat treatment; however, for the sake of simplicity, the expression “CEL2 scaffold” will be hereafter adopted, without further specifying the glass-ceramic nature of the sintered material.

Scaffold characterization

The scaffolds were chromium-coated and their morphology and porous 3-D architecture were investigated by scanning electron microscopy (Philips 525M; accelerating voltage = 15 kV). The inner porous network was also non-destructively investigated by micro-computed tomography (micro-CT; SkyScan 1174, Micro Photonics Inc.) to assess the pores characteristics. For the sake of comparison, the total porosity of the scaffolds was also calculated through mass-volume measurements as $(1-\rho_s/\rho_0)\times 100$, wherein ρ_s is the scaffold density (mass/volume ratio) and ρ_0 (g cm^{-3}) is the density of bulk material.

Biological assessment

Materials

MEM medium, foetal bovine serum (FBS), and the other reagents were purchased from Sigma (St. Louis, MO, USA). Gremlin was purchased from R&D Systems (Minneapolis, MN, USA).

Scaffold pre-treatment

The scaffolds (dimensions: 10.0 mm × 10.0 mm × 10.0 mm due to the shrinkage occurring upon heat treatment) were soaked in Tris-buffered simulated body fluid (SBF) [27] for 1 week to stimulate the formation of a HA layer, which is known to act as a biomimetic skin favouring cell adhesion. Before seeding cells, the SBF-treated scaffolds were sterilized with ultraviolet light exposure and preconditioned for 24 h in multiwells containing culture medium.

Cell culture conditions

Human osteoblast-like cell line, MG-63 (ATCC, Rockville, MD, USA), was grown in MEM medium containing 2 mM L-glutamine, 1% (v/v) antibiotic/antimycotic solution, 1 mM sodium pyruvate, and 10% (v/v) FBS in an atmosphere of 5% CO_2 and 95% air at 37 °C.

Treatment of cells with SWs

The SW generator utilized was a piezoelectric device (Piezoson 100, Richard Wolf, Knittlingen, Germany) designed for clinical use in orthopaedics and traumatology. The instrument generates focused underwater SWs at various frequencies (1 to 4 impulses/s) and intensities (0.05 to 1.48 mJ/mm^2). For medical use in orthopaedics, SWs of approximately 0.01 to 0.6 mJ/mm^2 are applied [28]. The experimental set-up has been described elsewhere [29]. Briefly, each cell-containing tube was placed vertically in the generator. The SW unit was held in contact with the tube by means of a water-filled cushion. Ultrasound gel was used as contact medium between cushion and tube. MG-63 cells (10^6/ml) were exposed to SWs at an energy level corresponding to 0.22 mJ/mm^2; 100 total impulses were used.

Cell growth within scaffolds and gremlin treatment

Cells were divided in the three experimental groups: 1) cells not exposed to SWs and not treated with gremlin (C); 2) cells exposed to SWs and not treated with gremlin (SW); 3) cells exposed to SWs and treated with gremlin (SW+G). For each experimental group, cells were seeded (90,000 cells) on the scaffolds and analysed on day 20 of treatment. Gremlin (0.9 μg/ml dissolved in PBS) was added to the cells of group 3 on alternate days. At the appropriate times, scaffolds were treated with trypsin/EDTA (0.25%/0.3%) to harvest the cells grown within them. Detached cells were used for the following determinations.

Cell count and viability

Cells were counted in a Burker chamber using a light microscope (Leitz, Wetzlar, HM-LUX, Germany). Viability was checked microscopically with the trypan blue exclusion test (dye concentration 0.8 mg/ml); 400 cells were counted for each sample and results were expressed as percentages of trypan blue-positive cells.

Evaluation of osteoblast activity parameters

After 20 days, cells detached from scaffolds of all experimental groups were examined for the assessment of osteoblast activity parameters. mRNA content of BMP-4, BMP-7, alkaline phosphatase (ALP), and osteocalcin (OCN) was determined by real-time PCR as reported elsewhere [23]. GAPDH was used as housekeeping gene. The sequences of forward and reverse primers are reported in Table 1. The fold change in mRNA content was defined as the relative expression compared to that of control cells, taken as 1, and calculated as $(2 - \Delta\Delta Ct)$, where $\Delta Ct = Ct_{sample} - Ct_{GAPDH}$ and $\Delta\Delta Ct = \Delta Ct_{sample} - \Delta Ct_{control}$.

Statistical analysis

All data are expressed as means ± SD of 3 different experiments. The significance of differences between group means was assessed by variance analysis, followed by the Newman-Keuls test ($p < 0.05$).

Results

Glass-ceramic scaffolds

Figure 1 shows the open-cells structure of a typical PU sponge, used as a sacrificial template for scaffolding, that exhibits a 3-D network of pores ranging from 200 up to 800 μm. The porosity of the PU foam, assessed by micro-CT measurements, was 90 vol.%; the mean strut thickness and the mean pore size were 84 μm and 580 μm, respectively. During the sponge replication process, the polymeric foam was coated with a thin and continuous layer of CEL2 particles in order to obtain, after the heat treatment, a glass-derived replica of the template (Figure 2). The total porosity of the scaffolds was estimated to be 69 vol.% by micro-CT analysis (Figure 3), that also revealed an excellent 3-D interconnectivity of the macropores (the open porosity was estimated to be above 95% of the overall porosity). The mean strut thickness and mean pore size were 101 μm and 445 μm, respectively; these values are comparable to those reported by other authors for human cancellous bone [30]. An extensive characterization of CEL2 scaffolds by micro-CT has been reported elsewhere by Renghini and co-workers [31,32]. Density assessment through mass-volume measurement substantially confirmed the assessments by micro-CT (total porosity of about 70 vol.%).

Biological tests

Figure 4 shows the effect of gremlin on the growth of human MG-63 cells exposed to SWs before seeding on the scaffolds. The significant decrease in cell numbers observed in SW-treated cells (–30%) in comparison with control cells was completely prevented by gremlin, which indeed somewhat increased cell numbers (+7%). Viability, evaluated by the trypan blue exclusion test, remained about 100% in all experimental groups (data not shown).

Figures 5 and 6 show the mRNA content of BMP-4, BMP-7, ALP and OCN in control cells, and in SW-exposed cells treated or not with gremlin. Compared to control cells, with regard to BMP-4

expression (Figure 5(a)), an 8.5-fold increase was observed in SW-exposed cells, whereas this induction decreased significantly (by 3.9 times) in cells grown in the presence of gremlin. With regard to BMP-7 expression (Figure 5(b)), the mRNA increase was completely blocked in the gremlin-treated cells; the content doubled in SW-treated cells, whereas it was similar to that of control cells in the presence of gremlin.

The effect of gremlin on ALP mRNA was similar to that on BMP-4 (Figure 6(a)). The increase due to SW exposure (4.6 times) was partially reduced by gremlin (1.7 times). In the case of OCN (Figure 6(b)) the effect of gremlin was more marked: the mRNA content of this osteogenic factor in cells exposed to SWs and maintained in the presence of BMP inhibitor was decreased in comparison with both SW-treated cells (–67%) and control cells (–53%).

Discussion

The use of absorbable biomaterials is often desirable in bone and dental surgery, so that the implant can be progressively replaced by new tissue while dissolving over time [33-36]. However, if strong and safe mechanical support to surrounding tissues and/or external loads is a goal, implantation of an absorbable material could be risky. CEL2 formulation was properly designed so that the resulting scaffolds have a very moderate tendency to resorption in aqueous media [30] (maintenance of structural integrity after implantation [12,26]) and good bioactive properties (formation of a HA layer on scaffold struts, which is a precondition for the development of a tight bond to host bone [32]). Furthermore, CEL2 scaffolds closely mimicked the foam-like structure of cancellous bone and exhibited well-densified and sound trabeculae. The porosity content is in the range recommended for bone tissue engineering scaffolds [37]. The presence of an open, highly interconnected 3-D porous network (as assessed through micro-CT analysis) is a key feature for bone tissue engineering applications, as the flow of culture medium containing cells during cell seeding throughout the scaffold is critical to develop an evenly populated tissue engineered

construct and it is fundamental that there are paths for cells to migrate, tissue to grow in and waste products to flow out *in vivo*.

An improved knowledge of the molecular mechanisms underlying the osteogenic properties of SWs could be important in order to expand their application in several medical fields, including orthopaedics and dental diseases characterized by marked bone loss. Muzio et al. reported elsewhere that the joint use of SWs and glass-ceramic macroporous scaffolds increases the activity of human osteoblast-like MG-63 cells, probably via increased expression of BMPs [23]. The present research confirms that SW-induced modulation of BMPs is a crucial event in improving osteogenic properties of MG-63 cells grown on scaffolds: in fact, the inhibition of the BMP activity by treatment with gremlin completely prevents the effects of SWs.

With regard to effects on cell growth, SW-treated cells exposed to gremlin show an increased proliferation rate versus controls, which confirms our previous suggestion that the reduced cell proliferation caused by SWs corresponds to an induction of cell differentiation, coupled with increased osteogenic activity of MG-63 cells [23]. This inverse correlation between cell growth and tissue-specific activity of the cells is in agreement with recent reports by other research groups, showing that in osteoblastic cells the growth arrest is accompanied by an increase of bone formation [38].

The results of this study are also in accordance with the observations by Chang et al. [39], who showed that BMP-4 induces G_0/G_1 arrest and differentiation in osteoblast-like cells, by increasing expression of $p21^{CIP}$ and $p27^{KIP1}$. These authors also evidenced a transient BMP-4-mediated increase in association of β_3-integrin with focal adhesion kinase and in Shc/ErK2, contributing to the SMAD1/5 phosphorylation. The involvement of ERK in the osteoblast differentiation signalling cascade has been also demonstrated in C3H10T1/2 mesenchymal progenitor cells, following BMP-2 inducement [40].

Figure 5 shows that the treatment with gremlin also decreased the expression of BMP-4 and BMP-7. It is known that gremlin exerts its potent inhibitory action by binding to and forming

heterodimers with BMP-2, BMP-4, and BMP-7; the binding of gremlin to selective BMPs prevents ligand-receptor interaction and subsequent downstream signalling [41]. It may be hypothesized that this effect is the consequence either of the gremlin-induced block of differentiation due to SW exposure, or of decreased expression of BMPs due to the lack of binding between BMPs and their receptors. In the present study, the effects over a 20-day period of analysis were investigated consistently to the experimental protocol adopted elsewhere [23,25]; looking at the future, experiments to investigate the expression of BMPs at early phases of SW-gremlin treatment and to determine the signalling pathways involved will be important to draw more definite conclusions.

The importance of increased BMP expression in mediating SW osteogenic properties is confirmed by the observation that, in gremlin-treated cells, the expression of both ALP and OCN is much lower than it is in SW-treated cells, and that the OCN value is below that of control cells. Some signalling transduction pathways activated by SWs and leading to the increased expression of BMPs can be postulated. Other authors reported elsewhere that SWs are able to induce ERK phosphorylation [42,43]. Interestingly, phosphorylated ERK1/2 by fluid shear stress mediates the expression of osteogenic genes via activation of BMPs/mothers against decapentaplegic (Smad) pathway acting through NF-κB and regulating Runx2 expression [44]. Finally, low-intensity pulsed ultrasounds affect phosphorylation of Smad transcription factors; phosphorylated Smads enter the nucleus and function as effectors of BMP signalling by regulating transcription of specific genes involved in osteogenic differentiation [45].

In addition, SWs could act as a physical stimulus at the plasma-membrane level, inducing changes in protein or lipid components and, as a consequence, modulating BMP transcription. If SWs have an effect on polyunsaturated fatty acid (PUFAs) of membrane phospholipids, this could modulate the amount of ligands available for peroxisome proliferator-activated receptors (PPARs); ligand-activated transcription factors regulate several metabolic pathways, including osteogenesis. Future investigations to assess the amount of free PUFAs and the changes occurring to PPARs in SW-

treated cells will be useful to clarify the possible importance of this metabolic pathway in increasing BMP expression.

Conclusions and perspectives

Glass-ceramic scaffolds mimicking the architectural characteristics of cancellous bone were successfully fabricated by the sponge replication technique and used as porous substrates for *in vitro* biological investigations using osteoblast-like cells. It was shown the direct and essential involvement of increased BMP expression in the osteogenic effect of SWs, thus improving current knowledge of the molecular mechanisms underlying the osteogenic properties of this type of physical stimulation on bone formation. Looking at future applications, it is worth underlining the clinical importance of having tissue engineered scaffolds with a high bone regenerative potential to be associated to BMP-mediated osteogenic stimulation due to SW exposure. This combination could be used as a promising alternative to loading implantable scaffolds with recombinant human BMPs, which would result in a significant reduction of medical costs.

Acknowledgments

The work was supported by grants from Regione Piemonte and University of Turin, Italy.

Conflict of interest

The authors confirm that there are no conflicts of interest.

References

[1] Kaihara, S and Vacanti JP. Tissue engineering: toward new solutions for transplantation and reconstructive surgery. *Arch Surg* 1999; 134: 1184-1188.

[2] MacNeil S. Biomaterials for tissue engineering of skin. *Mater Today* 2008; 11: 26-35.

[3] Kock L, Van Donkelaar CC and Ito K. Tissue engineering of functional articular cartilage: the current status. *Cell Tissue Res* 2012; 347: 613-627.

[4] Amini AR, Laurencin CT and Nukavarapu SP. Bone tissue engineering: recent advances and challenges. *Crit Rev Biomed Eng* 2012; 40: 363-408.

[5] Schlickewei W and Schlickewei C. The use of bone substitutes in the treatment of bone defects - the clinical view and history. *Macromol Symp* 2007; 253: 10-23.

[6] Jones JR and Hench LL. Regeneration of trabecular bone using porous ceramics. *Curr Opin Solid State Mater Sci* 2003; 7: 301-307.

[7] Baino C and Vitale-Brovarone C. Three-dimensional glass-derived scaffolds for bone tissue engineering: current trends and forecasts for the future. *J Biomed Mater Res A* 2011; 97: 514-535.

[8] Tan L, Yu X, Wan P and Yang K. Biodegradable materials for bone repairs: a review. *J Mater Sci Technol* 2013; 29: 503-513.

[9] Patel PJ, Rees HC and Olver JM. Fibrovascularization of porous polyethylene orbital floor implants in humans. *Arch Ophthalmol* 2003; 121: 400-403.

[10] Dorozhkin SV. Bioceramics of calcium orthophosphates. *Biomaterials* 2010; 31: 1465-1485.

[11] Nam SB, Bae YC, Moon JS and Kang YS. Analysis of the postoperative outcome 405 cases of orbital fracture using 2 synthetic orbital implants. *Ann Plast Surg* 2006; 56: 263-267.

[12] Baino F, Ferraris F, Bretcanu O, Verné E and Vitale-Brovarone C. Optimization of composition, structure and mechanical strength of bioactive 3-D glass-ceramic scaffolds for bone substitution. *J Biomater Appl* 2013; 27: 872-890.

[13] Hench LL, Splinter RJ, Allen WC and Greenlee TK. Bonding mechanisms at the interface of

ceramic prosthetic materials. *J Biomed Mater Res* 1971; 2: 117-141.

[14] Wang CJ, Chen HS, Chen CE and Yang KD. Treatment of non-union fracture of the long bone with shock waves. *Clin Orthop* 2001; 387: 95-101.

[15] Romp JD, Rosendahl T, Schollner C and Theis C. High-energy extracorporeal shock wave treatment of nonunions. *Clin Orthop* 2001; 387: 102-111.

[16] Marasaki K, Schmizu H, Beppu M, Aoki H, Takagi M and Takashi M. Effect of extracorporeal shock waves on callus formation during bone lengthening. *J Orthop Sci* 2003; 8: 474-481.

[17] Shrivastava SK and Kailash. Shock wave treatment in medicine. *J Biosci* 2005; 30: 269-275.

[18] Wang CJ, Yang KD, Ko JY, Huang CC, Huang HY and Wang FS. The effects of shockwave on bone healing and systemic concentrations of nitric oxide (NO), TGF-beta1, VEGF and BMP-2 in long bone non-unions. *Nitric Oxide* 2009; 20: 298-303.

[19] Wang CJ, Wang FS, Yang KD, Weng LH, Hsu CC, Huang CS and Yang LC. Shock wave therapy induces neovascularization at the tendon-bone junction. A study in rabbits. *J Orthop Res* 2003; **21**: 984-989.

[20] Martini L, Giavaresi G, Fini M, Torricelli P, Borsari V, Giardino R, De Pretto M, Remondini D and Castellani GC. Shock wave therapy as an innovative technology in skeletal disorders: study on transmembrane current in stimulated osteoblast-like cells. *Int J Artif Organs* 2005; 28: 841-847.

[21] Chen YJ, Wurtz T, Wang CJ, Kuo YR, Yang KD, Huang HC and Wang FS. Recruitment of mesenchymal stem cells and expression of TGF-beta 1 and VEGF in the early stage of shock wave-promoted bone regeneration of segmental defect in rats. *J Orthop Res* 2004; 22: 526-534.

[22] Hofmann A, Ritz U, Hessmann MH, Alini M, Rommens PM and Rompe JD. Extracorporeal shock wave-mediated changes in proliferation, differentiation, and gene expression of human osteoblasts. *J Trauma Inj Inf Crit Care* 2008; 65: 1402-1410.

[23] Muzio G, Vernè E, Canuto RA, Martinasso G, Saracino S, Brignone S, Miola M, Berta L,. Frairia R and Vitale-Brovarone C. Shock waves induce activity of human osteoblast-like cells in bioactive scaffolds. *J Trauma Inj Inf Crit Care* 2010; 68: 1439-1444.

[24] Duarić L, Cvek SZ, Cvijanović O, Santić V, Marić I, Crncević-Orlić Z, Bobinac D. Expression of the BMP-2, -4 and -7 and their antagonists gremlin, chordin, noggin and follistatin during ectopic osteogenesis. *Coll Antropol* 2013; 37: 1291-1298.

[25] Vitale-Brovarone C, Verné E, Robiglio L, Appendino P, Bassi F, Martinasso G, Muzio G and Canuto R. Development of glass-ceramic scaffolds for bone tissue engineering: characterisation, proliferation of human osteoblasts and nodule formation. *Acta Biomater* 2007; 3: 199-208.

[26] Vitale-Brovarone C, Baino F and Verné E. High strength bioactive glass-ceramic scaffolds for bone regeneration. *J Mater Sci Mater Med* 2009; 20: 643-653.

[27] Kokubo T and Takadama H. How useful is SBF in predicting in vivo bone bioactivity? *Biomaterials* 2006; 27: 2907-2915.

[28] Ogden JA, Alvarez RG, Levitt R and Marlow M. Shock wave therapy (Orthotripsy) in muscoloskeletal disorders. *Clin Orthop* 2001; 387: 22-40.

[29] Frairia R, Catalano MG, Fortunati N, Fazzari A, Raineri M and Berta L. High energy shock waves (HESW) enhance paclitaxel cytotoxicity in MCF-7 cells. *Breast Cancer Res Treat* 2003; 81: 11-19.

[30] Macdonald HM, Nishiyama KK, Kang J, Hanley DA and Boyd SK. Age-related patterns of trabecular and cortical bone loss differ between sexes and skeletal sites: a population-based HR-pQCT study. *J Bone Mineral Res* 2011; 26: 50-62.

[31] Renghini C, Komlev V, Fiori F, Verné E, Baino F and C. Vitale-Brovarone. Micro-CT studies on 3-D bioactive glass-ceramic scaffolds for bone regeneration. *Acta Biomater* 2009; 5: 1328-1337.

[32] Renghini C, Giuliani A, Mazzoni S, Brun F, Larsson E, Baino F, Vitale-Brovarone C. Microstructural characterization and in vitro bioactivity of porous glass-ceramic scaffolds for bone regeneration by synchrotron radiation X-ray microtomography. *J Eur Ceram Soc* 2013; 33: 1553-1565.

[33] Kuboki Y, Ku S, Yoshimoto R, Kaku T, Takita H, Li D, Kokai Y, Yunoki S, Sammons RL; Ozeki K, Miyata T. Calcified honeycomb-shaped collagen maintains its geometry in vivo and effectively induces vasculature and osteogenesis. *Nano Biomedecine* 2009; 1: 85-94.

[34] Kuboki Y, Yagami K, Iku S, Kaku T, Terada M, Kitagawa Y, Takita H, Li D, Kimura M, Sammons RL. Geometry of extracellular matrix: optimal tunnel size for bone formation in disk-form honeycomb β-TCP. *Nano Biomedicine* 2010; 2: 107-113.

[35] Saito E, Saito A, Kuboki Y, Kimura M, Honma Y, Takahashi T, Kawanami M. Periodontal repair following implantation of beta-tricalcium phosphate with different pore structures in class III furcation defects in dogs. *Dental Mater J* 2012; 31: 681-688.

[36] Saito A, Saito E, Kuboki Y, Kimura M, Nakajima T, Yuge F, Kato T, Honma Y, Takahashi T, Ohata N. Periodontal regeneration following application of basic fibroblast growth factor-2 in combination with beta tricalcium phosphate in class III furcation defects in dogs. *Dental Mater J* 2013; 32: 256-262.

[37] Karageorgiou V and Kaplan D. Porosity of 3D biomaterial scaffolds and osteogenesis. *Biomaterials* 2005; 26: 5474-5491.

[38] Datta NS, Kolailat R, Fite A, Pettway G and Abou-Samra AB. Distinct roles for mitogen-activated protein kinase phosphatase-1 (MKP-1] and ERK-MAPK in PTH1R signaling during osteoblast proliferation and differentiation. *Cell Signal* 2010; 22: 457-466.

[39] Chang SF, Chang TK, Peng HH, Yeh YT, Lee DY, Yeh CR, Zhou J, Cheng CK, Chang CA and Chiu JJ. BMP-4 induction of arrest and differentiation of osteoblast-like cells via p21 CIP1 and p27 KIP1 regulation. *Mol Endocrinol* 2009; 23: 1827-1838.

[40] Lou J, Tu Y, Li S and Manske PR Involvement of ERK in BMP-2 induced osteoblastic differentiation of mesenchymal progenitor cell line C3H10T1/2. *Biochem Biophys Res Commun* 2000; 268: 757-762.

[41] Wordinger RJ, Zode G and Clark AF. Focus on molecules: gremlin. *Exp Eye Res* 2008; 87: 78-79.

[42] Wang FS, Wang CJ, Chen YJ, Chang PR, Huang YT, Sun YC, Huang HC, Yang YJ, Yang KD. Ras induction of superoxide activates ERK-dependent angiogenic transcription factor HIF-1alpha and VEGF-A expression in shock wave-stimulated osteoblasts. *J Biol Chem* 2004; 279: 10331-10337.

[43] Chen YJ, Kuo YR, Yang KD, Wang CJ, Sheen Chen SM, Huang HC, Yang YJ, Yi-Chih S, Wang FS. Activation of extracellular signal-regulated kinase (ERK) and p38 kinase in shock wave-promoted bone formation of segmental defect in rats. *Bone* 2004; 34: 466-477.

[44] Liu L, Shao L, Li B, Zong C, Li J, Zheng Q, Tong X, Gao C, Wang J. Extracellular signal-regulated kinase1/2 activated by fluid shear stress promotes osteogenic differentiation of human bone marrow derived mesenchymal stem cells through novel signaling pathways. *Int J Biochem Cell Biol* 2011; 43: 1591-1601.

[45] Yang Z, Ren L, Deng F, Wang Z, Song J. Low-intensity pulsed ultrasound induces osteogenic differentiation of human periodontal ligament cells through activation of bone morphogenetic protein-Smad signaling. *J Ultrasound Med* 2014; 33: 865-873.

Figure legends

Figure 1. PU sponge used as a sacrificial template: (a) SEM micrograph (magnification 50×) and (b) micro-CT reconstruction of the porous polymer structure.

Figure 2. CEL2 scaffold: (a) digital camera picture of the obtained cuboid after heat treatment (950 °C/3 h) and (b) SEM micrograph of the interconnected porous architecture of the scaffold (magnification 300×).

Figure 3. Micro-CT analysis of CEL2 scaffold: (a) 3-D reconstruction of a scaffold sub-volume (dimensions about 5 mm × 2 mm × 2 mm) and (b) mid-length cross-sections in the [xy], [xz] and [yz] orthogonal planes.

Figure 4. Osteoblasts grown in scaffolds after exposure to SWs and treatment with gremlin. Data are expressed as mean ± SD of 3 different experiments. Means with different letters are significantly different from one another ($p = 0.0064$) as determined by analysis of variance followed by *post-hoc* Newman-Keuls test. Labels: C = control cells; SW = cells exposed to SWs; SW + G = cells exposed to SWs and treated with gremlin.

Figure 5. mRNA content of BMP-4 and BMP-7 in osteoblasts grown in scaffolds after exposure to SWs and treatment with gremlin. Data are expressed as mean ± SD of 3 different experiments. For each panel, means with different letters are significantly different from one another ($p < 0.05$) as determined by analysis of variance followed by *post-hoc* Newman-Keuls test. Labels: C = control cells; SW = cells exposed to SWs; SW + G = cells exposed to SWs and treated with gremlin.

Figure 6. mRNA content of alkaline phosphatase (ALP) and osteocalcin (OCN) in osteoblasts grown in scaffolds after exposure to SWs and treatment with gremlin. Data are expressed as mean ± SD of 3 different experiments. For each panel, means with different letters are significantly different from one another ($p < 0.05$) as determined by analysis of variance followed by *post-hoc* Newman-Keuls test. Labels: C = control cells; SW = cells exposed to SWs; SW + G = cells exposed to SWs and treated with gremlin.

Table 1. Forward and reverse primer sequences for real-time PCR analysis.

Gene Access Number	Sequence FW: forward primer; RV: reverse primer	Annealing (°C)	Cycles
GAPDH NM_002046	FW-5'-GTC GGA GTC AAC GGA TTT GG-3' RV-5'-GGG TGG AAT CAT ATT GGA ACA TG-3'	52	30
ALP NM_000478	FW-5'-CTC CCA GTC TCA TCT CCT-3' RV–5'-AAG ACC TCA ACT CCC CTG AA-3'	58	40
Osteocalcin NM_199173	FW-5'-GTG ACG AGT TGG CTG ACC-3' RV–5'-CAA GGG GAA GAG GAA AGA AGG-3'	59	35
BMP-7 NM_001719	FW-5'-GTG GAA CAT GAC AAG GAA T-3' RV-5'-GAA AGA TCA AAC CGG AAC-3'	58	40
BMP-4 D30751	FW-5'-CTC GCT CTA TGT GGA CTT C-3' RV-5'-ATG GTT GGT TGA GTT GAG G-3'	58	45

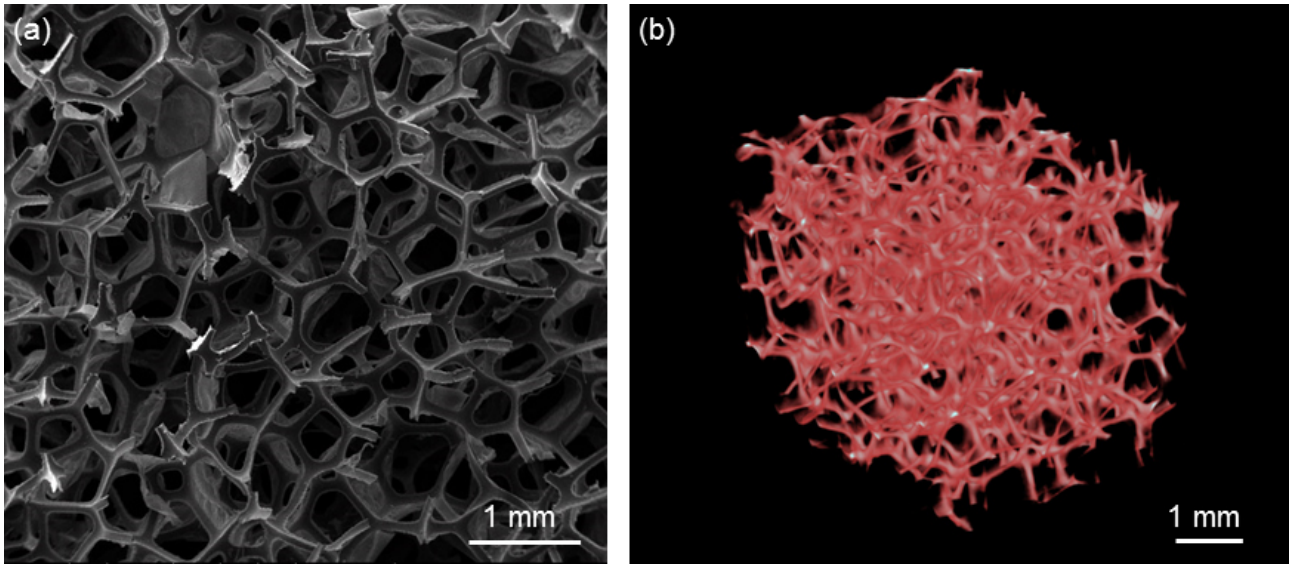

Fig. 1

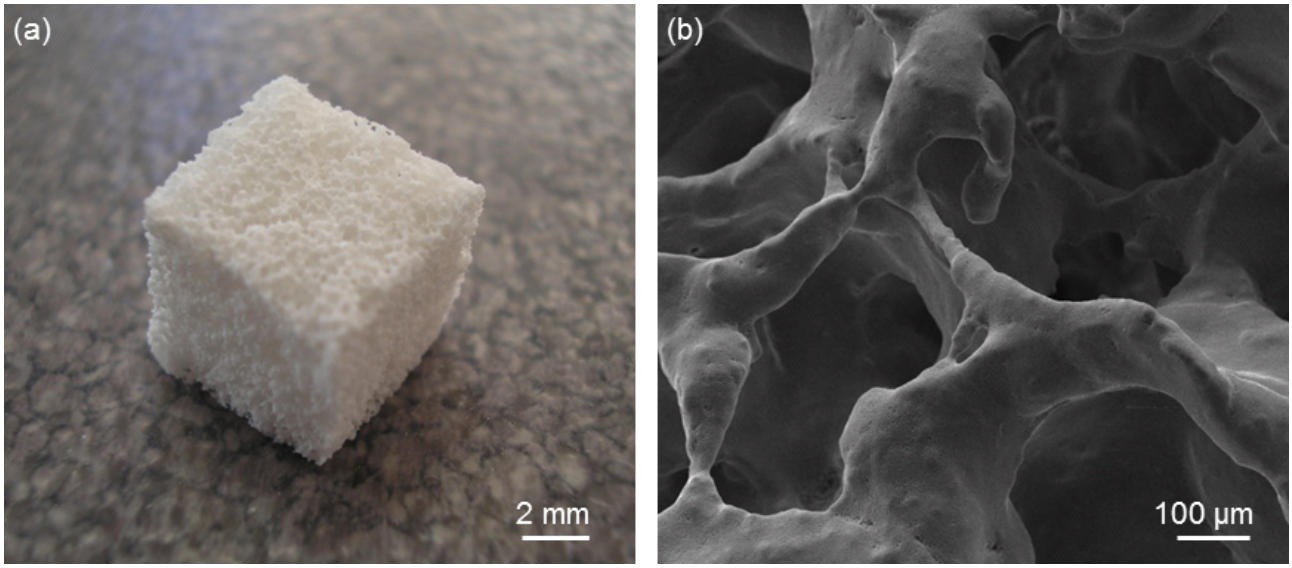

Fig. 2

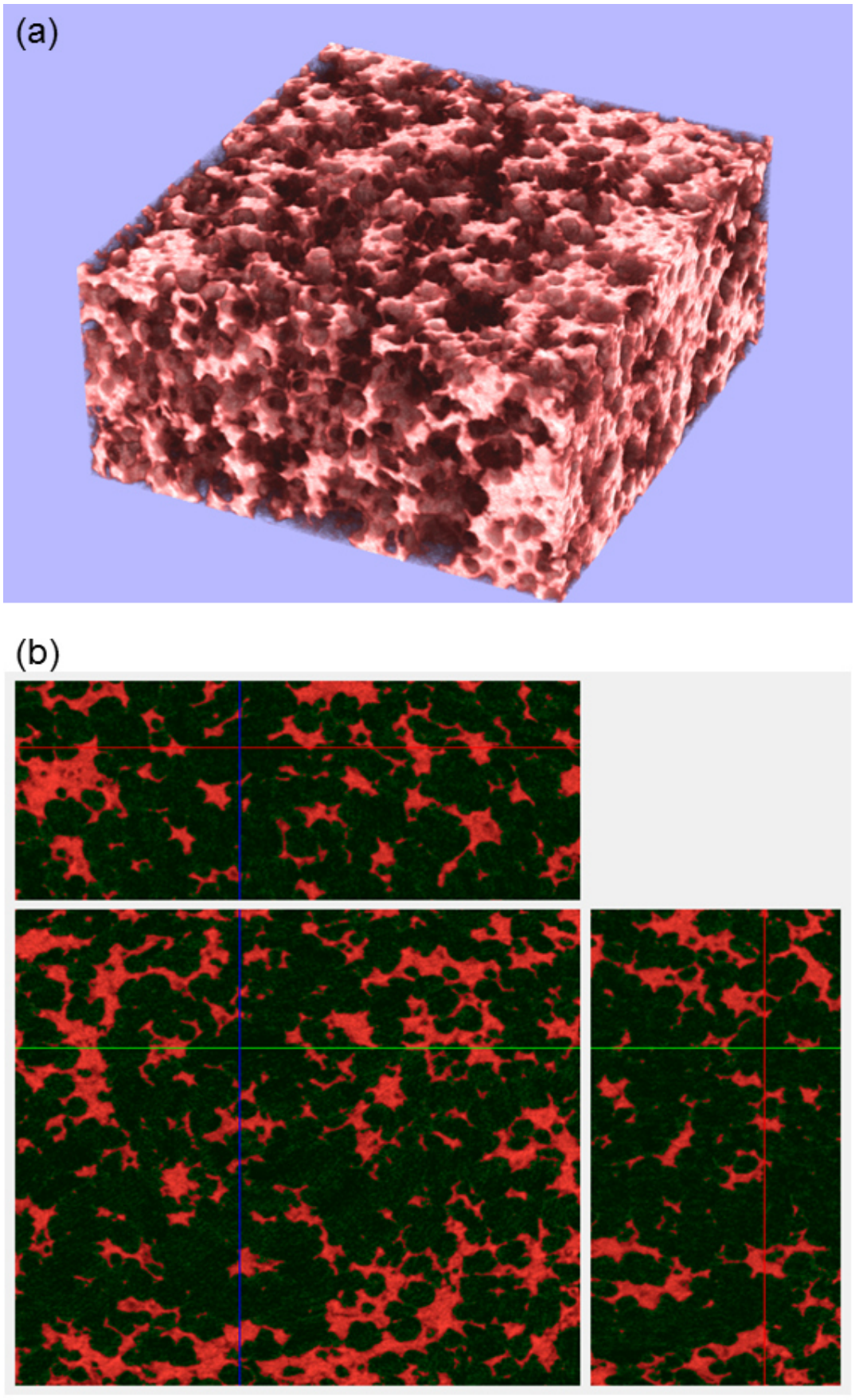

Fig. 3

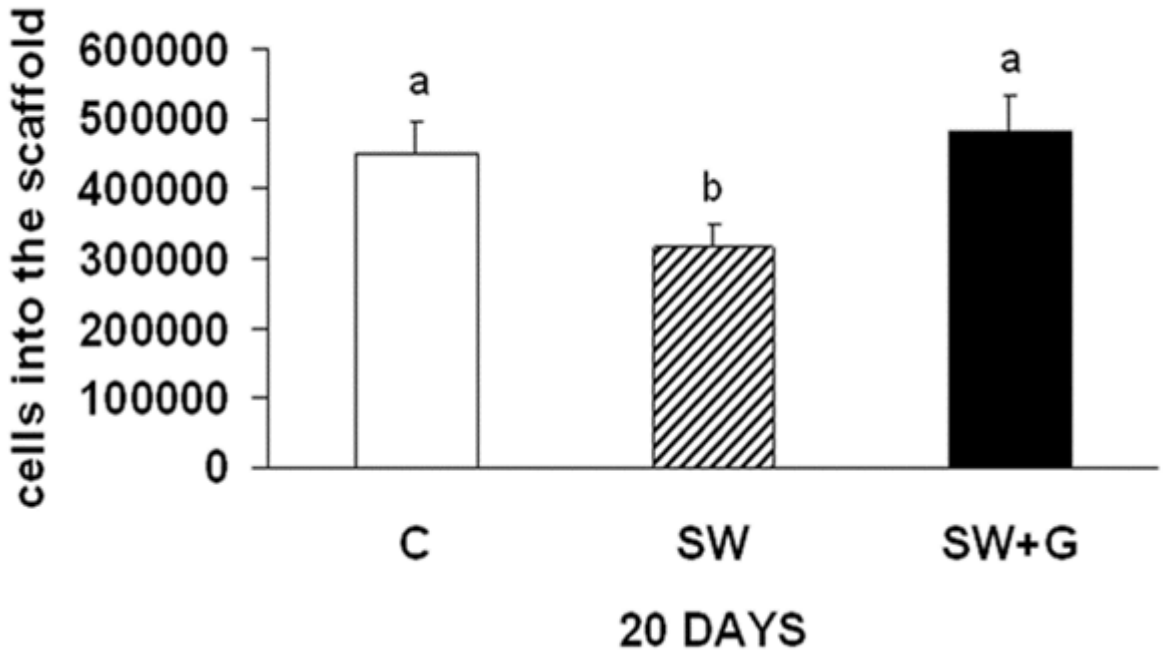
cells into the scaffold
600000
500000
400000
300000
200000
100000
0
a
b
a
C
SW
SW+G
20 DAYS

Fig. 4

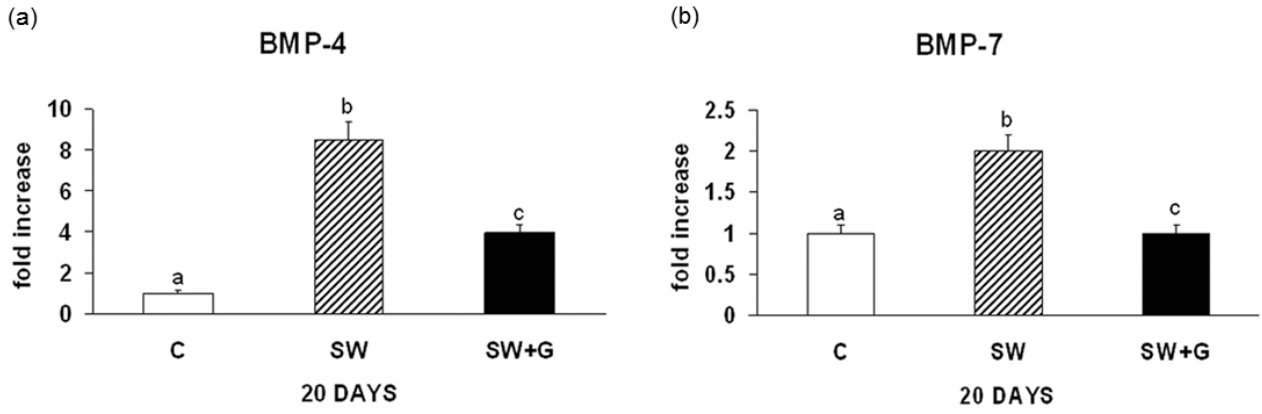
(a)
BMP-4
fold increase
10
8
6
4
2
0
a
b
c
C
SW
SW+G
20 DAYS
(b)
BMP-7
fold increase
2.5
2
1.5
1
0.5
0
a
b
c
C
SW
SW+G
20 DAYS

Fig. 5

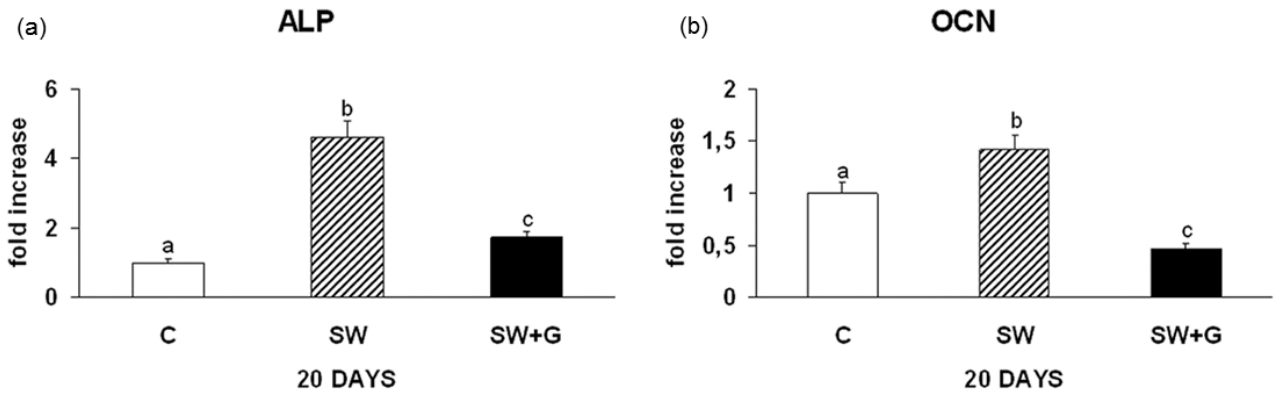
(a)
ALP
fold increase
6
4
2
0
a
b
c
C
SW
SW+G
20 DAYS
(b)
OCN
fold increase
2
1,5
1
0,5
0
a
b
c
C
SW
SW+G
20 DAYS

Fig. 6